48.8 mW Multi-cell InP HBT Amplifier with on-wafer power combining at 220 GHz

Thomas B. Reed, Mark J. W. Rodwell
Department of Electrical and Computer Engineering
University of California
Santa Barbara, CA, USA 93106
treed@ece.ucsb.edu

Zach Griffith, Petra Rowell, Miguel Urteaga,
Mark Field, Jon Hacker
Teledyne Scientific and Imaging, LLC
1049 Camino Dos Rios
Thousand Oaks, CA, USA 91360
zgriffith@teledyne-si.com

***Abstract*— We report 220 GHz Solid State Power Amplifier (SSPA) using a 250nm Indium Phosphide HBT technology. Amplifiers reported include designs having 2 and 4 power combined cells. The 4-cell amplifiers exhibited 10 dB small signal gain and 48.8 mW of output power with 4.5 dB gain at 220 GHz. These amplifiers have a 3-dB small signal bandwidth of greater than 48 GHz. A 5-µm thick BCB microstrip wiring environment with 4 levels of interconnects allowed for low-loss transmission lines, mm-wave tuning structures, and dense interconnects within each cell. The 2-cell amplifiers provide 10.9 dB small signal gain at 220 GHz with a 3-dB bandwidth of greater than 42 GHz and 26.3 mW of saturated output power at 208GHz.**

Keywords-InP HBT, MMIC, Power amplifier, On-wafer power combining

I. INTRODUCTION

Solid-state Power Amplifiers (SSPA) operating above 220 GHz are needed for future communications and imaging systems, both as transmitter elements in phased array transmitters and as driver amplifiers for higher-power vacuum tube power amplifiers. Significant output power is necessary to overcome the high atmospheric attenuation above 100 GHz associated with rain, humidity, and fog. To date, the highest reported output power for a solid state G-band (140-220 GHz) power amplifier is an InP HEMT power amplifier having 50mW of saturated output power between 217 and 220 GHz [1] in a waveguide-block package. An early reported G-band power amplifier, implemented using InP HEMTs, provided 20mW saturated output power between 176 and 189GHz [2]. A G-band medium power amplifier using InP HBTs produced greater than 8mW saturated output power at 190 GHz [3]. 300 GHz medium power amplifiers have been reported using 256-nm InP HBTs [4].

Power combining with multiple gate or emitter fingers is necessary for high saturated output power. On-wafer 4-1 and 2-1 power combiners have been demonstrated in a microstrip wiring environment at 95 GHz resulting in 427-mW of output power in a HEMT power amplifier [5]. 4-1 combiners at 220GHz were realized with similar Dolph-Chebyshev structures using coplanar waveguide in the amplifier reported in [1]. Additionally, a 206-294GHz mHEMT amplifier [6] has been demonstrated using an identical non-inverted, shielded, thin-film microstrip environment with dense interconnect vias as the amplifiers reported here.

State-of-the-art InP HBTs at the 250nm technology node have demonstrated the requisite device bandwidths and gains for amplifiers at high-mm-, sub-mm-wave frequencies [7]. While 250nm InP DHBTs have much higher off-state breakdown compared to state-of-the-art InP HEMTs [8], the usable voltage and current handling (to form the load-line of a power amplifier cell) of these technologies, where the MAG/MSG is appreciable, is similar. A closer examination of the MAG/MSG of a cascode cell formed with these technologies at high-mm-wave frequencies shows that the InP HBT cell yields many more dB of gain compared to its InP HEMT counterpart. Additionally, for demonstration of a power amplifier at these same frequencies, low-loss interconnect and power splitters/combiners are essential. The use of a multi-layer, thin-film, substrate shielded non-inverted microstrip environment using low-loss BCB (ε_r = 2.7) available in InP

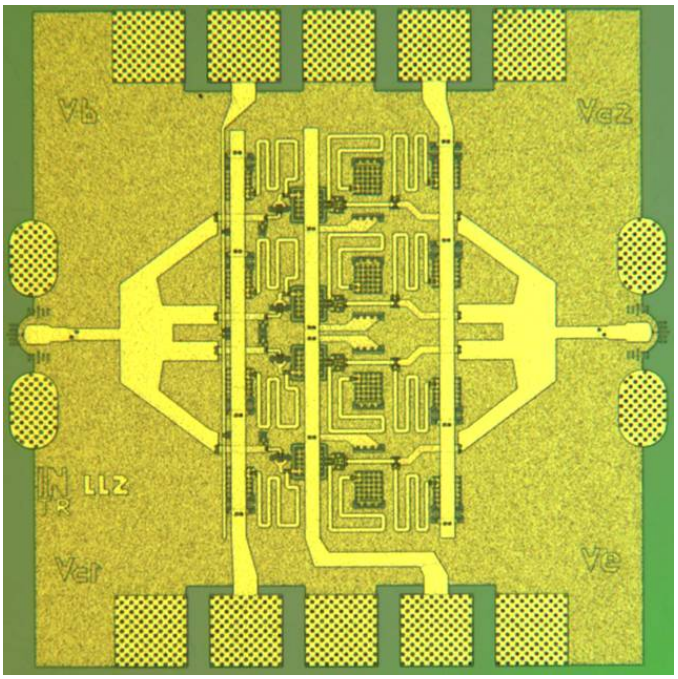

Figure 1. 4-cell InP HBT amplifier with 4-1 power combiners. The die is 0.7x0.65 mm^2.

This work was supported under the Defense Advanced Research Projects Agency (DARPA) HiFive program.

978-1-61284-712-2 /11/$26.00 ©2011 IEEE

HBT processes allows very compact HBT PA cells and combiner networks to be formed with much lower loss compared to similar networks formed in grounded coplanar waveguide (G-CPW) interconnect on thinned InP substrates, used in InP HEMT processes.

Here we report a state-of-the-art, 4-cell InP HBT solid-state power amplifier (SSPA) exhibiting 10 dB small signal gain and 48.8 mW of saturated output power with 4.5dB gain at 220 GHz. The amplifier has a 3-dB bandwidth greater than 48 GHz. We also report a 2-cell amplifier demonstrating 10.9 dB small signal gain at 220 GHz with a 3-dB bandwidth greater than 42 GHz, with 26.3 mW of saturated output power at 208GHz. At 220GHz, this is the highest RF output power for an SSPA reported to date in an InP HBT technology.

II. Indium Phosphide HBT Process

For the power amplifiers here reported, a 250nm InP technology having ~4.5V breakdown voltage was used. The peak bandwidth of a single HBT was f_{max} = 700GHz and f_τ = 400GHz. At the quiescent HBT bias used in the amplifiers (I_c = 5.5mA/μm^2 and V_{ce} = 2V), a single HBT shows f_{max} = 590GHz and f_τ = 350GHz. The PA HBT cells used in the amplifiers were composed of 4-emitter fingers, with L_e = 6-μm. The PA cell is compact, with footprints of 18x7.5μm^2 for common emitter and 16x9μm^2 for common base configuration. At the quiescent amplifier bias, the PA cells exhibit f_{max} = 530GHz and f_τ = 333GHz, showing that the parasitics associated with the cell assembly do little to reduce the available bandwidth and gain of the PA cell.

A 4-metal layer interconnect is used. The inter-metal interconnect separation by BCB (ε_r = 2.7) is 1.0um. The process supports the use of compact, stacked interconnect vias for the first, second, and third interconnect levels. MIM capacitors (SiN_x, 0.3fF/μm^2) are formed between the first and second level interconnect metal, and 50-Ω/sq thin-film resistors are available. Further details of the 250nm device and interconnect technology have been reported in [4,9].

III. MMIC Power Amplifier Design

The amplifier IC design was simulated using Advanced Design System (ADS) and an Agilent-HBT model for the 250nm HBT technology. Thin-film, low-loss microstrip wiring is used in the designs. All transmission line structures, MIM capacitors, device feed structures, and probe pads were simulated using the ADS Momentum 2.5-D electromagnetic simulator. The thin-film microstrip is formed by using the top-most interconnect (MET-4) for signal, while the first-metal interconnect (MET-1) is used to form a large ground-plane (5um MET-1 to MET-4 separation), as well as shield the signal lines from the high-ε_r ~ 12.8 InP substrate. This interconnect scheme prevents the excitation of unwanted substrate modes and permits the use of wider, lower loss wiring for a given interconnect Z_o.

The multi-cell amplifiers use a basic high gain cascode cell constructed using one 4-finger common emitter and one 4-finger common-base HBT. DC bias to the cell was provided through quarter-wave microstrip chokes. High cell gain was achieved by impedance matching the input of the cascode stage to 50Ω. To maintain a compact IC layout, port impedances were matched using MIM capacitors as capacitive elements and high Z_o transmission lines as inductive elements for an operating frequency of 220GHz.

Maximum output power in each cell was achieved by matching the output impedance to a load line maintained within the high performance operating area of the common-base PA cell. This operating area is the region of I_c vs. V_{cb} curve defined by the collector-emitter saturation voltage, the device's maximum current density, the safe operating power density, the common-base breakdown voltage, and the variation of f_τ with collector voltage. DC bias for the PA was set at J_c = 5mA/μm^2, while design variations were produced at biases of V_{cb} = 1, 1.25, and 1.5 V for the common-base cell.

The goal of power combining was to create a series of SSPAs that could provide up to 50 mW of output power to a

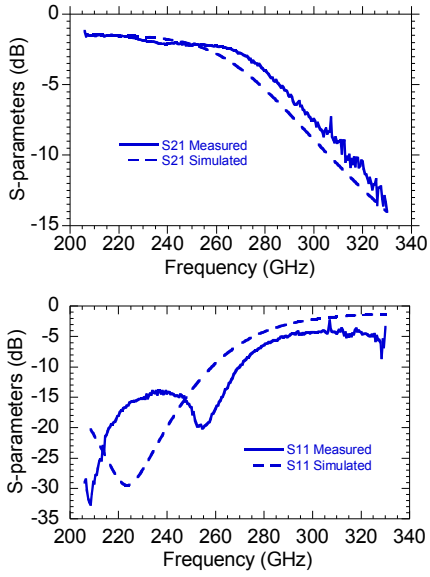

Figure 2. Insertion Loss (Top Left) and Return Loss (Bottom Left) for back-to-back 4-1 combiners. Each combiner has less than 1 dB Insertion Loss at 220 GHz.

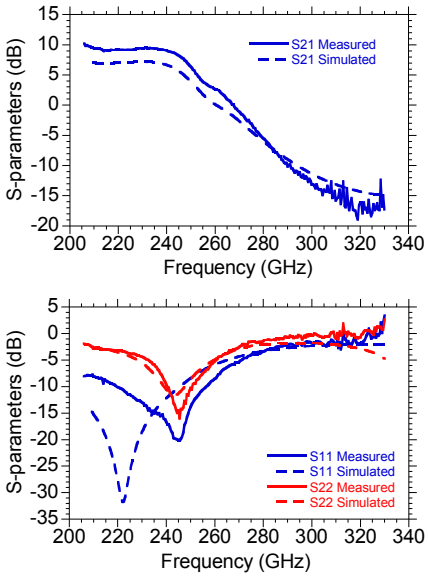

Figure 3. Power Gain, S21 of a 4-Cell Power Amplifier (Top Center) with 10dB small signal gain at 220 GHz. Return Loss, S11 and S22 of 4-Cell Power Amplifier (Bottom Center).

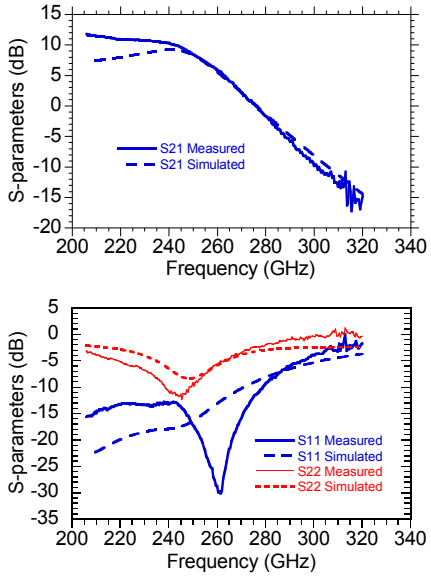

Figure 4. 2-Cell Power Amplifier S-parameters. S21 (Top Right) shows 10.9dB gain at 220GHz. The S11 and S22 plot (Bottom Right) shows input and output return loss.

load. To create the 2- and 4-cell amplifiers, both a 2-1 ¼ λ_g combiner and a 4-1 Dolph-Chebyshev combiner were designed in 5-µm BCB microstrip. The resulting 4-1 splitter/combiner appears as a wedge on the input and output in Fig. 1. The ¼ λ_g , high-Z_o 2-1 combiners are shown at input and output in Fig. 6.

The 4-1 combiner provides a 50Ω load impedance to the each of 4 tuned cascode cells while matching to the 50Ω impedance of the load at 220 GHz. The combiner consists of a high-Z_o transmission line less than ¼ λ_g feeding a central point. A small MIM capacitor is added there to tune the EM structure for low loss at 220 GHz. A 2.5-D EM-simulator was used to verify the center frequency of the combiner structures. A measured result of two back-to-back 4-1 combiners is shown in Fig. 2. The insertion loss per one side 4-1 combiner is 0.75dB and the insertion loss per one side 2-1 combiner is 0.6dB.

The 2-1 power combiner used a quarter-wave 70Ω impedance transformer to turn Z_o at the cell output into $2Z_o$ at the combining point, creating a 50Ω match to the output. The 2-1 power combiner was verified using a 2.5-D EM-simulator. This combiner was used in the 2-cell amplifier.

IV. Experimental Results

The SSPA MMIC was tested for small-signal gain using an Agilent 8510C Vector Network Analyzer (VNA) and WR-3 Oleson Microwave Laboratory frequency extending heads. Probe tip LRRM calibration performed by WinCal XE was used to obtain measurements of S-parameters with the reference plane at the probe pads of the IC [10].

The small signal gain of the 4-cell amplifier is shown in Fig. 3. With I_{c1} = 132mA, I_{c2} = 132mA, V_{c2} = 1.80 V, V_{c1} = 2.1V, V_{e2} = -4.2V, and V_{b1} = 2.10 V, the measured gain at 220 GHz was 10.1dB. The 3dB bandwidth extends from 206GHz to 254GHz.

The 2-cell amplifier results shown in Fig. 4 was biased at I_{c1} = 66mA, I_{c2} = 66mA, V_{c2} = 1.85 V, V_{c1} = 2.1V, V_{e2} = -4.1V, and V_{b1} = 1.82 V. The measured gain, as shown in Fig. 4, at 220 GHz is 10.9dB with a local maximum of 11.8dB at 206 GHz with S21 dropping 3dB below peak at 248 GHz.

Output Power measurements were taken using a 40 GHz signal generator, followed by a VDI WR-05 200 GHz multiplier chain and waveguide probes for sweeping power at 208GHz. The resulting output power was measured through a WR-05 waveguide probe, WR-05 waveguide extension, a WR-05 to WR-10 waveguide transition and into an Erickson PM4 sub-millimeter wave power meter. The detected power was then calibrated for the insertion loss of the output probe and waveguide. For measurements from 210 to 227GHz, a VDI WR-04 220GHz multiplier chain was used in a similar setup with a WR-04 waveguide transition. Power measurements above 225GHz were limited by source output power.

For P_{in} vs. P_{out} measurements, the 4-cell amplifier was biased under the same conditions as for RF testing. The 4-cell SSPA had an output power of 48.8mW and a gain of 4.5 dB at 220 GHz. See Fig. 7 for 220 GHz power sweep results. Fig. 8 shows output power and gain vs. frequency. Results show that

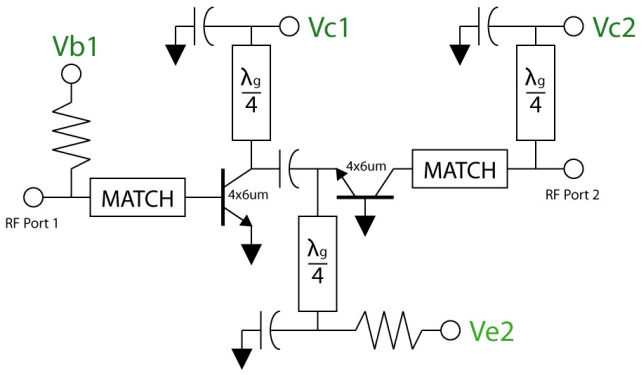

Figure 5. Schematic diagram of a single power amplifier cell.

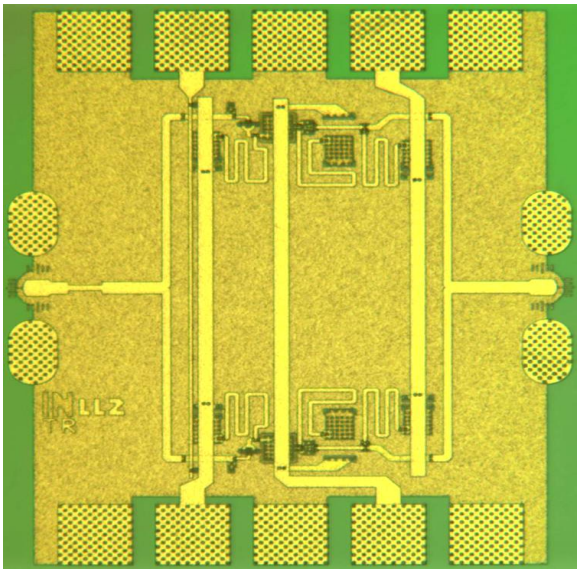

Figure 6. 2-Cell Power Amplifier with 2-to-1 power combining. The die is 0.7x0.58 mm^2.

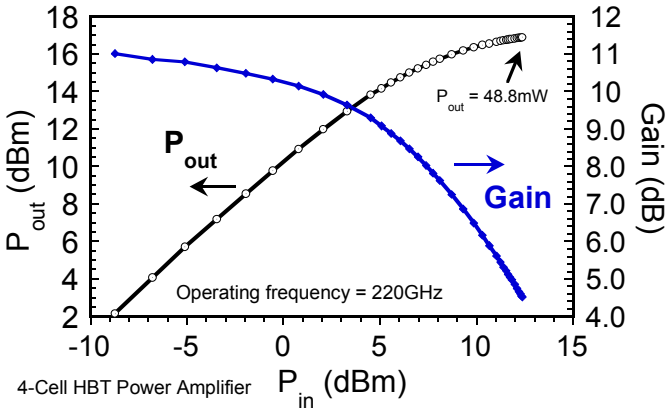

Figure 7. Measured Gain and Output Power vs. Input Power for a 220 GHz 4-Cell Power Amplifier.

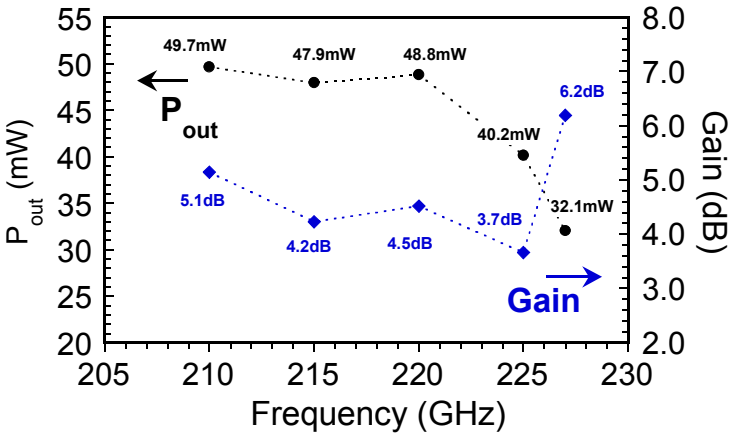

Figure 8. Measured Maximum Output Power and associated gain vs. frequency for a 220 GHz 4-Cell Power Amplifier. The maximum amplifier P_{out} at a given frequency is limited by the source power.

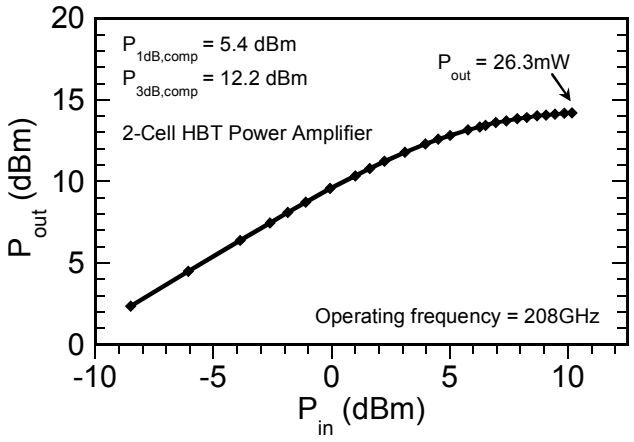

Figure 9. 2-Cell Power Out vs. Power In at 208 GHz.

the 4-cell amplifier can produce greater than 48mW of output power over 210-220GHz. In power testing, the 2-cell amplifier was held at the same bias as for RF testing. 26.3mW of saturated output power was measured at 208GHz. The power sweep for the 2-Cell Amplifier is shown in Fig. 9.

ACKNOWLEDGMENT

This research was supported under the Defense Advanced Research Projects Agency (DARPA) Hi-Five program. Program support was provided by Dr. John Albrecht, Program Manager, at the DARPA Microsystems Technology Office. The authors would like to thank Teledyne Scientific for fabrication of this MMIC and Vibhor Jain and Hyunchul Park for guidance.

REFERENCES

[1] V. Radisic, K.M.K.H. Leong, X. Mei, S. Sarkozy, W. Yoshida, P.-H. Liu, J. Uyeda, R. Lai, and W.R. Deal, "A 50mW 220GHz Power Amplifier Module," *2010 IEEE Microwave Symposium Digest*, July 2010, pp. 45-48.

[2] P.-P. Huang, R. Lai, R. Grundbacher, and B. Gorospe, "A 20-mW G-band monolithic driver amplifier using 0.07-µm InP HEMT," *IEEE MTT-S Digest*, San Francisco, CA, June 2006, pp. 806-809.

[3] V.K. Paidi, Z. Griffith, W. Yun, M. Dahlstrom, M. Urteaga, N. Parthasarathy, S. Munkyo, L. Samoska, A. Fung, and M.J.W. Rodwell, "G-band (140-220GHz) and W-band (75-110 GHz) InP DHBT medium power amplifiers," *IEEE Trans. Microwave Theory Tech*., vol. 53, no. 2, pp. 598-605, Feb. 2005.

[4] J. Hacker, S. Munkyo, A. Young, Z. Griffith, M. Urteaga, T. Reed, and M. Rodwell, "THz MMICs based on InP HBT Technology," Microwave Symposium Digest (MTT), *2010 IEEE MTT-S International*, pp.1126-1129, May 2010.

[5] Y.C. Chen, D.L. Ingram, R. Lai, M. Barsky, R Grunbacher, T. Block, H.C. Yen, D.C. Streit, "95-GHz InP HEMT MMIC amplifier with 427-mW power output," *IEEE Microwave and Guided Wave Letters*, vol. 8, no. II, Nov. 1998, pp. 399-401.

[6] Z. Griffith, W. Ha, P. Chen, D-H. Kim, B. Brar, "A 206-294GHz 3-stage Amplifier in 35nm InP mHEMT Using a Thin-Film Microstrip Environment", *Proc. IEEE International Microwave Symposium*, Anaheim, CA, May 23-28, 2010.

[7] M. Rodwell, M. Le, B. Brar, "InP Bipolar ICs: Scaling Roadmaps, Frequency Limits, Manufacturable Technologies", *Proceedings of the IEEE*, vol. 96, no. 2, Feb. 2008.

[8] R. Lai, W. Deal, X. Mei, W. Yoshida, J. Lee, L. Dang, J. Wang, Y. Kim, P. Liu, V. Radisic, M. Lange, T. Gaier, L. Samoska, A. Fung, "Fabrication of InP HEMT devices with extremely high Fmax", *Conf. Proc. IEEE Indium Phosphide and Related Materials*, Versailles, France, May 25-29, 2008.

[9] M. Urteaga, R. Pierson, P. Rowell, M.J. Choe, D. Mensa, B. Brar, "Advanced InP DHBT Process for High Speed LSI Circuits", *Conf. Proc. IEEE/LEOS Indium Phosphide and Related Materials*, Versailles, France, May 25-29, 2008.

[10] Rumiantsev, A.; Sweeney, S.L.; Corson, P.L.; , "Comparison of on-wafer multiline TRL and LRM+ calibrations for RF CMOS applications," *ARFTG Microwave Measurement Symposium*, 2008 72nd, pp.132-136, 9-12 Dec. 2008.